MOLECULAR ECOLOGY

Molecular Ecology (2016) doi: 10.1111/mec.13780

Body mass-corrected molecular rate for bird mitochondrial DNA

BENOIT NABHOLZ,* ROBERT LANFEAR† and JÉROME FUCHS‡

*Institut des Sciences de l'Evolution, UMR 5554, Université Montpellier place Eugène Bataillon, Montpellier Cedex 5 34095, France, †Department of Biological Sciences, Faculty of Science, Macquarie University, Sydney, NSW 2109, Australia, ‡Institut de Systématique, Évolution, Biodiversité, ISYEB-UMR 7205 CNRS, MNHN, UPMC, EPHE, Muséum National d'Histoire Naturelle, Sorbonne Université, 57 rue Cuvier, CP5175005, Paris, France

Abstract

Mitochondrial DNA remains one of the most widely used molecular markers to reconstruct the phylogeny and phylogeography of closely related birds. It has been proposed that bird mitochondrial genomes evolve at a constant rate of ~0.01 substitution per site per million years, that is that they evolve according to a strict molecular clock. This molecular clock is often used in studies of bird mitochondrial phylogeny and molecular dating. However, rates of mitochondrial genome evolution vary among bird species and correlate with life history traits such as body mass and generation time. These correlations could cause systematic biases in molecular dating studies that assume a strict molecular clock. In this study, we overcome this issue by estimating corrected molecular rates for birds. Using complete or nearly complete mitochondrial genomes of 475 species, we show that there are strong relationships between body mass and substitution rates across birds. We use this information to build models that use bird species' body mass to estimate their substitution rates across a wide range of common mitochondrial markers. We demonstrate the use of these corrected molecular rates on two recently published data sets. In one case, we obtained molecular dates that are twice as old as the estimates obtained using the strict molecular clock. We hope that this method to estimate molecular rates will increase the accuracy of future molecular dating studies in birds.

Keywords: birds, body mass, mitochondrial, molecular clock

Received 7 February 2016; revision accepted 22 July 2016

Introduction

Mitochondrial DNA is widely used to reconstruct the timescale of bird evolution using molecular dating. The divergence times obtained from this approach have been used to examine the impact of life history, geology, climate and biogeography on the diversification of birds (e.g. Avise & Walker 1998; Weir *et al.* 2009; Lanfear *et al.* 2010). However, the molecular dating methods used to derive the timescale of bird evolution remain controversial.

Most molecular dating studies use a combination of fossil calibrations and relaxed molecular clocks to infer divergence times from molecular data. Fossil calibrations provide information on the divergence times of some nodes in the phylogeny, and relaxed molecular clocks allow divergence times of other nodes to be estimated while allowing for variation in substitution rates among lineages. However, the fossil record is scarce or completely lacking for most bird families and genera (Mayr 2009, 2013). Consequently, molecular dating studies in birds often rely on strict molecular clocks, assuming a single substitution rate that does not (or to a limited extent) vary over time and among lineages. This approach allows molecular dates to be estimated entirely in the absence of fossil calibrations. The most frequently employed method is the use of a divergence rate of 2% per million years (Myr). This rate was proposed some time ago (Brown *et al.* 1979; Shields &

Correspondence: Benoit Nabholz, Fax: +33 4 67 14 36 22; E-mail: benoit.nabholz@umontpellier.fr

Wilson 1987; Fleischer *et al.* 1998), and recently reaffirmed by Weir & Schluter (2008) in a widely cited analysis in which they estimated a divergence rate of 2.1% per million years (0.0105 subst/site/myr) for mitochondrial cytochrome *b* sequences in birds.

Although convenient, the use of strict molecular clocks in birds remains controversial (García-Moreno 2004; Lovette 2004; Pereira & Baker 2006; Ho 2007; Nabholz *et al.* 2009; Nguyen & Ho 2016). Widespread variation in rates of molecular evolution among species is not only predicted on empirical grounds (e.g. Lehtonen & Lanfear 2014), but has also been repeatedly confirmed in empirical studies of birds (Pereira & Baker 2006; Nabholz *et al.* 2009; Eo & DeWoody 2010; Pacheco *et al.* 2011; Jarvis *et al.* 2014; Nguyen & Ho 2016). Indeed, the broader picture is that variation in substitution rates is the rule rather than the exception across the tree of life (Bromham *et al.* 1996; Nabholz *et al.* 2008; Welch *et al.* 2008; Thomas *et al.* 2010; Lourenço *et al.* 2013; Qiu *et al.* 2014). Failing to account for this variation may lead to systematically biased estimates of divergence times in molecular dating studies. For example, if large birds tend to evolve more slowly than smaller birds, then the use of the 'standard' strict molecular clock would lead to underestimates of divergence times for largest birds and overestimates of divergence times for smallest birds.

Across clades as diverse as vertebrates and angiosperms, substitution rates have repeatedly been shown to correlate with life history traits such as body mass, longevity and generation time (Bromham 2009). In birds, it has been shown that substitution rates in both the nuclear and mitochondrial genomes correlate with life history traits (Nabholz *et al.* 2009; Jarvis *et al.* 2014) and species richness (Eo & DeWoody 2010; Lanfear *et al.* 2010). These correlations suggest that the variation in substitution rates among bird species is, to some extent at least, predictable. This presents opportunities to circumvent the problem of using strict molecular clocks, because one might be able to use commonly measured life history traits, such as body size, to estimate variation in substitution rates among species. Using this approach, one could define a 'corrected' molecular clock that accounts for some of the known variation in substitution rates among lineages, even in the absence of fossil calibrations.

In this study, we used the complete or nearly mitochondrial genome of 475 bird species to produce a collection of corrected molecular rates for birds. We focus on body mass because it is known for most extant species of bird (Dunning 2007), and so provides the most convenient life history trait from which to estimate corrected molecular rates for molecular dating studies. Conveniently, body mass could also be extrapolated using allometric relationship with skeletal measurements (e.g. Campbell & Marcus 1992; Field *et al.* 2013). We provide corrected molecular rates for third codon positions, as well as for total substitution rates for each of the individual mitochondrial genes that are commonly used for molecular dating in birds. We hope that these corrected molecular rates will increase the accuracy of future molecular dating studies in birds.

Materials and methods

Sequences, alignments and topology

We downloaded all of the complete or near-complete mitochondrial genomes available on NCBI/GenBank (http://ncbi.nlm.nih.gov) in May 2015, resulting in a data set for 487 species. When multiple individuals were available per species, we selected the longest and/or the highest quality sequence (as inferred from the number of uncertainty codes). When all sequences were deemed to be of equal quality, we selected an individual randomly. We aligned the 12 H-stranded protein-coding genes (i.e. all the protein-coding genes except NADH dehydrogenase 6, ND6) using BIOEDIT (Hall 1999), after excluding all nucleotides from the stop codons. We carefully checked all alignments by eye. We excluded 12 dubious sequences during alignment, resulting in alignments of 475 species (see Table S1, Supporting information).

We estimated a maximum-likelihood topology using RAXML (Model GTR+G; Stamatakis 2014). We used a constrained topology to follow Prum *et al.* (2015) (using option '-g' in RAXML) regarding the basal neoavian relationships. We also repeated our analyses using a topology following Jarvis *et al.* (2014) who gave similar results. The topology and the alignments are available at Dryad doi:10.5061/dryad.1040d.

Life history traits

We obtained body mass data from Dunning (2007). When body mass was not available for a species, we used the median body mass of the genus in Dunning (2007) except if another species of the same genus was available in our data set. Otherwise, we left that species' body mass unknown. For example, body mass for the black-browed bushtit (*Aegithalos bonvaloti*) was not present in Dunning (2007), but we left its body mass as unknown in our data set because another *Aegithalos* (the long-tailed bushtit, *Aegithalos caudatus*), for which a mass is available, is present in our data set. Using this approach, we obtained body mass estimates for 435 of the 475 species in our alignments.

Substitution rate estimation

To derive the most accurate molecular rate estimates across species, we used a two-step approach inspired by Nabholz *et al.* (2008, 2009). This approach allows us to make the best use of the relatively few and relatively old reliable fossil calibrations in birds (Benton *et al.* 2009; Ksepka & Clarke 2015), while still estimating rates of evolution for fast-evolving mitochondrial DNA sequences which typically would not be used together with such old fossil calibrations. First, we estimated molecular divergence dates using amino acid alignment and fossil-based calibrations (see 'Molecular dating'). Second, we used molecular divergence dates to calibrate the species-specific substitution rate of nucleotide sequences. An outline of the method is presented in Fig. S1 (Supporting information).

To limit the effect of saturation, we defined monophyletic groups of sequences for which the maximal nucleotide divergence between any given pair of species was lower than 0.4 subst/site. To do this, we used a custom R script built with the APE package (Popescu *et al.* 2012; R Core Team 2013), which led to 84 independent monophyletic clades containing a total of 436 species. Inspection of a saturation plot (a plot of phylogenetic divergences against the uncorrected pairwise genetic divergences) indicated that saturation was moderate at 0.4 subst/site. A threshold set at 0.3 subst/site gave similar results.

Within each group, substitution rates were estimated using MCMCTREE (Yang & Rannala 2006; Rannala & Yang 2007) implemented in PAML 4 (Yang 2007). We applied an HKY model of substitution with an autocorrelated relaxed clock model. We choose the HKY model because it is the most complex model currently implemented in MCMCTREE. The analysis of each group was calibrated using three estimates of the divergence date of the most recent common ancestor of each group obtained from the molecular dating analysis based on amino acid sequences: the mean divergence date, the minimum 95% credibility interval of the divergence date and the maximum 95% credibility interval of the divergence date. Using these three dates allows us assess the effects of the uncertainty of our divergence dates on our molecular rate estimates. The maximum 95% CIs provide minimal age estimates and therefore maximal substitution rate estimates for each group, while the minimum 95% CIs provide maximal age estimates and therefore minimal substitution rate estimates for each group. Because several groups contained only two sequences, we added an out-group to all clades defined as the most closely related species in the phylogeny. For example, a clade contained the two *Halcyon* species (*Halcyon pileata, Halcyon sancta*), and we used the Pied Kingfisher (*Ceryle rudis*) sequence as out-group. This out-group was used to help in the estimation of substitution rates for in-group sequences. Substitution rate estimates for out-groups were not used in downstream analyses, because they were occasionally quite divergent from in-group sequences and so prone to issues associated with saturation.

Molecular dating

The molecular dating analyses using amino acid sequences were performed with PHYLOBAYES version 4.1 (Lartillot *et al.* 2009) using the default site-heterogeneous mixture model (CAT) and a log-normal autocorrelated relaxed clock (option -ln) (Thorne *et al.* 1998). Autocorrelated relaxed clocks have been shown to outperform other relaxed-clock models (Lepage *et al.* 2007). The priors on divergence dates were uniform (Lepage *et al.* 2007). We ran two chains in parallel for at least 20 000 steps for all the analyses, with a burn-in of 10 000 steps. In all cases, the two chains gave similar results, suggesting that the MCMC analyses had converged. Convergences was also assessed visually and using 'tracecomp' ensuring that the discrepancy statistic *d* between estimates parameters were below 0.4 for most parameters.

For the calibrations, we relied exclusively on fossils, in order to avoid potential problems linked to calibrations based on geographic distributions (Heads 2005, 2011). We particularly avoided the controversial calibration based on the vicariance of New Zealand to calibrate the first split within the Passeriformes (Trewick & Gibb 2010; Mayr 2013; Gibb *et al.* 2015). Although less controversial, more recent biogeographic calibrations have been used to date the diversification of the Hawaiian honeycreepers (Lerner *et al.* 2011). We chose to not use these calibrations but instead use them as an independent source of information to evaluate our analyses.

As the placement of some calibrations is ambiguous, we choose to test several combinations of fossil calibrations summarized in Table 1, and discuss specific cases here. The Anseriformes fossil *Vegavis iaai*, found in the Maastrichtian, would seem to provide a clear minimum bound for the Neognathae/Paleognathae split (Benton *et al.* 2009; Ksepka & Clarke 2015). However, we chose to not consider *V. iaai* as an Anseriformes because its phylogenetic placement is ambiguous (Mayr 2009, 2013). For the maximum bound of the Neognathae/Paleognathae split, we followed the proposition of Benton *et al.* (2009) and set it at 86.5 Myr. Alternatively, *Gansus yumenensis* from the early Cretaceous of China (110 Myr) was used by Jetz *et al.* (2012), whereas Jarvis *et al.* (2014) used the maximum boundary of the Upper Cretaceous (99.6 Myr).

Table 1 Fossil calibration combinations used in molecular dating analyses

Calibration sets	Taxon 1	Taxon 2	Maximum bound (Myr)	Minimum bound (Myr)
1, 2, 4	Neognathae	Paleognathae	86.5	66
3	Neognathae	Paleognathae	110	66
1, 2, 3, 4	Anseriformes	Galliformes	Free	66
1, 2, 3, 4	Sphenisciformes	Procellariiformes	Free	60.5
1, 2, 3, 4	Coraciidae	Alcedinidae	Free	51.57
1, 2, 3, 4	Apodidae	Trochilidae	Free	51
1	Psittaciformes	Passeriformes	Free	53.5
2, 3, 4	Psittaciformes	Passeriformes	65.5	53.5
4	Oscines	Suboscines	34	28

The other minimum-bound calibrations we used in our molecular dating analysis all followed the suggestions of Ksepka & Clarke (2015). Additionally, we constrained the Passeriformes/Psittaciformes split between 53.5 and 65.5 Myr based on the first Eocene fossil of Australia (Boles 1997) and on the stem Psittaciformes fossil *Pulchrapollia gracilis* (Prum *et al*. 2015). The maximum bound at 65.5 Myr was used in all analyses except calibration set 1 (see Table 1; Longrich *et al*. 2011; Prum *et al*. 2015). Finally, in one analysis (calibration set 4), we constrained the Oscines/Suboscines split between 28 and 34 Myr based on the first Suboscines from early Oligocene (28 Myr, Mayr & Manegold 2006) and on the Eocene/Oligocene limit (34 Myr). This later maximum bound relies on the fact that all Passeriformes fossils known from the Eocene are stem Passeriformes; therefore, crown Oscines and Suboscines may have appeared latter during the Oligocene (Mayr & Manegold 2004; Mayr 2013).

To compare the results obtained using the four different calibration sets we propose (Table 1), we selected five divergence dates within the phylogeny (Table 2) for which we have independent evidence with which to assess the accuracy of our own analyses: (i) the first divergence within the extant Hawaiian honeycreeper which was inferred to occur 6 Myr (Lerner *et al*. 2011); (ii) the Sittidae (represented by *Sitta*)/Troglodytidae (represented by *Henicorhina* and *Campylorhynchus*) split for which the maximum bound is provided by the early Miocene (20.5–18 Myr) fossil of a Certhioidea (a clade containing the Sittidae and Certhidae) (Manegold 2007); (iii) the Oscines/Suboscines split for which a maximum bound is provided by the first Suboscines fossils (~28 Myr) (Mayr & Manegold 2006); (iv) the Stercorariidae/Alcidae split; and (v) the Jacanidae/other Scolopaci split; for both (iv) and (v), Smith (2015) provides minimum calibration points that could be compared with our analyses (Table 2).

Corrected rate model

All the statistical analyses were performed with R (R Core Team 2013). In the linear regression, body mass and substitution rates were log-transformed (logarithm of base 10) and parameters of the linear model were estimated using the R formula $\mathrm{lm}(\log_{10}(\mathrm{Rate}) \sim \log_{10}(\mathrm{Mass}))$. We repeated this analysis accounting for the relatedness among species using phylogenetic generalized least squares (Grafen 1989; Garland *et al*. 2000), and phylogenetic independent contrast (PIC; Felsenstein

Table 2 Comparison of molecular dating analyses with independent fossils or independent analysis. Mean dates are indicated and 95% CI are provided within parentheses

# Calibration sets	Hawaiian honeycreepers	Oscines/Suboscines	Sittidae/Troglodytidae	Stercorariidae/Alcidae	Jacanidae/other Scolopaci
Minimum fossil bound (Myr)	6	28	18	34.2	30
1	15.8 (12.1, 19.9)	63.9 (57.8, 69.9)	35.2 (29.9, 40.6)	47.9 (39.6, 56.5)	41.8 (32.2, 51.4)
2	13.4 (10.1, 16.9)	57.1 (54.9, 59.1)	30.3 (26.7, 33.6)	43.9 (35.8, 49.4)	37.6 (28.7, 46.0)
3	14.3 (10.9, 18.0)	57.4 (55.1, 59.3)	31.6 (27.3, 35.3)	42.7 (36.4, 48.9)	36.9 (28.1, 45.5)
4*	7.2 (5.8, 8.8)	33.9 (33.5, 34.0)*	19.0 (17.3†, 21.0)	41.2 (34.9, 46.5)	35.1 (26.6†, 42.3)

*In this analysis, the Oscines/Suboscines split was constrained to occur between 28 and 34 Myr.
†Indicates values that are in conflict with the fossil records.

1974), implemented in APE (Paradis 2011). However, the parameters estimated using these methods could not be used to obtain corrected substitution rates using an independent species' body mass.

Substitution rate variation among protein-coding genes

To test for variation in substitution rates among different protein-coding genes, we performed additional molecular dating analyses for all genes individually, except for the very short ATP8 and ND4L genes. This led to an additional 20 molecular dating analyses: all codon positions and third codon positions for each of 10 protein-coding genes individually. For each of these analyses, we estimated the branch lengths using the F84 model implemented in BASEML (Yang 2007). We did not use the HKY model here because we could not optimize it using BASEML on some data sets. However, the F84 model is conceptually similar to the HKY model used in MCMCTREE analyses. To avoid overparametrization due to the short alignments, we fixed the value of the kappa parameter (the transition-to-transversion ratio) to the value estimated using the whole data set ($\kappa = 8$). We also used the gamma distribution of rate variation among sites only in the analyses using all codon positions. We obtained substitution rates by dividing the terminal branch lengths by the appropriate divergence times estimated in the molecular dating analyses. In this case, very small branches can be associated with extremely high variance; we therefore excluded branch lengths shorter than 0.01 substitution per site. The same sets of species were analysed for every gene, meaning that if a species has a branch shorter than 0.01 for one particular gene, it was excluded for all, leading a set of $N = 292$ species. We did not use MCMCTREE for these analyses because many of these individual-gene data sets were small and the MCMC chain failed to converge.

To statistically compare substitution rates among protein-coding genes, we used an ANOVA with single-factor repeated-measures design with a model reflecting that the genes are nested within the 84 independent monophyletic clades (R formula: lm(Rate ~ Gene + Gene: Clade)). We also tested a model were Clade was a random effect (R formula: lme(Rate ~ Gene, random = ~1| Clade/Gene)). Finally, we tested the rate differences between each pair of genes using pairwise *t*-tests with adjusted *P*-values using a Bonferroni correction.

Working examples

We applied our method to two recently published data sets including relatively large and small birds. The first data set was composed of 16 ND1 sequences of *Circus* harriers (body mass ~500 g; Oatley *et al.* 2015). For this analysis, we used the phylogenetic tree estimated from these sequences in the original study (fig. 2 of Oatley *et al.* 2015).

The second dataset was composed of CYTB and ND2 sequences of the Buff-throated Woodcreeper complex (genus *Xiphorhynchus*, body mass ~40 g; Rocha *et al.* 2015). We restricted the analysis to one sequence per taxon (as presented in appendices A and B of Rocha *et al.* 2015) leading to a total of 11 sequences. As above, we used the phylogenetic tree estimated from these sequences in the original study (fig. 1 of Rocha *et al.* 2015).

In both examples, sequences were aligned using muscle (Edgar 2004) and checked by eye. Sites containing missing data were excluded. Branch lengths were estimated exclusively from the third codon position. We applied a molecular clock model in BASEML (model F84, kappa parameter fixed to 8.0, parameter 'clock = 1'). Then, we scaled the branch lengths of the tree using the body mass-corrected substitution rate for each clade (i.e. a single scalar is used for the entire tree). Finally, we estimated branch lengths from all codon positions for both data sets to compare our estimates with the commonly used 2% per Myr strict molecular clock rate. Alignments, phylogenies and the R script to convert branch lengths to divergence dates are provided at Dryad doi:10.5061/dryad.1040d.

Results

Molecular dating

Most fossil-based calibrations available are relatively deep in the bird phylogeny (Benton *et al.* 2009; Jarvis *et al.* 2014; Ksepka & Clarke 2015; Prum *et al.* 2015) and are not suited to the fast-evolving nucleotide sequences of the mitochondrial genome (Nguyen & Ho 2016). To make use of these ancient calibrations, we performed a molecular dating analysis with the amino acid sequences because they are less prone to saturation (Brown *et al.* 1982). We used four sets of calibrations (Table 1) reflecting the current uncertainty surrounding fossil calibrations for molecular dating analyses of birds. We also tested two topologies reflecting alternative hypotheses regarding the basal neoavian divergences (Jarvis *et al.* 2014; Prum *et al.* 2015). We obtain very similar dates between topologies (results not shown). Hereafter, we present only the results obtained using the Prum *et al.* (2015) topology.

Globally, the calibration sets 1, 2 and 3 provide very similar divergence dates that are all compatible with independent fossil data (Table 2). The Oscines/

Suboscines divergences are, however, 30–35 Myr older than the first known fossils (Mayr & Manegold 2004; Mayr 2013). Our analyses also provide divergence dates that are more than twice as old as the dates of Lerner *et al.* (2011) for the diversification of Hawaiian honeycreepers (Table 2).

Calibration set 4 provides younger dates than the other calibration sets, particularly within the Passeriformes. This is expected as this analysis includes an additional calibration bound that constrained Oscines/Suboscines split to occur between 28 and 34 Myr. This is about half the age of this split recovered with other calibration sets that do not calibrate this node (Table 2). This analysis provided dates that are in agreement with those of Lerner *et al.* (2011), but the minimum 95% credibility intervals (CI) are younger than the fossils records for the Sittidae/Troglodytidae split and for the Jacanidae/other Scolopaci split although the discrepancy is modest (Table 2, 17.3 vs. 18 Myr and 26.6 vs. 30 Myr, respectively).

It is difficult to favour one analysis over the others; therefore, we choose to consider both calibration set 2 (which is representative of the sets 1, 2 and 3) and calibration set 4 for the following analyses.

A mass-corrected molecular rate

We selected 84 independent monophyletic groups containing a total 437 species (Table S2, Supporting information). These groups match a criterion of limited divergence to accurately estimate substitution rates. Substitution rates were calibrated for each group using divergence dates obtained from the molecular dating using the fossil calibration sets 2 and 4 (see Materials and methods). Hereafter, we will refer to them as 'analysis 2' and 'analysis 4', respectively.

For analysis 2, the median third codon substitution rate was 0.0142 subst/sites/Myr (min = 0.0035, max = 0.0306). For analysis 4, the median third-codon substitution rate was 0.0165 subst/site/Myr (min = 0.0042, max = 0.0566). In both cases, the substitution rate varies by more than one order of magnitude among species.

To compare our approach with the widely used divergence rate of 0.01 substitutions per site per million years, which was originally estimated from all codon positions, we also inferred substitution rates using all codon positions. For analysis 2, the median substitution rate was 0.0035 subst/site/Myr (min = 0.0010, max = 0.0090) with all species having a rate below 0.01. For analysis 4, the median substitution rate was 0.0042 subst/site/Myr, but the distribution obtained overlapped extensively with the 0.01 (min = 0.0011, max = 0.0158). The passerines, for example, have a median substitution rate that is very close to it (median = 0.009 subst/site/Myr).

Both third codon and all position substitution rates are strongly negatively correlated with body mass (Table 3). The R^2 values are higher when substitution rates are estimated from third codon positions (0.46 and 0.60 for the analyses 2 and 4, respectively, Fig. 1) than when they are estimated from all codon positions (0.35 and 0.51 for the analyses 2 and 4, respectively). We speculate that this could result from the effects of natural selection on substitution rates. These effects are likely to be stronger on codon positions 1 and 2 than on third codon positions, and may weaken the relationship between body mass and substitution rates. However, regardless of the cause of the higher R^2 for third codon positions, it implies that body mass is a better predictor of third codon position substitution rates than substitution rates derived from all codon positions. As such, body mass-corrected rates will be more accurate if they are derived using substitution rates estimated from third codon positions only, and so we focus on deriving corrected rates for third codon positions only.

Both the GLS and PIC analyses, which control for phylogenetic nonindependence among species, confirmed a significant negative correlation between substitution rate and body mass (Table S3, Supporting information), demonstrating that the relationship between body mass and substitution rates is robust to control of the phylogenetic relationship among species. A similar conclusion was made by Nabholz *et al.* (2009).

The slope and the intercept of the linear models comparing third codon position substitution rates and body

Table 3 Parameter of the linear model: $\log_{10}$(Rate) ~ $\log_{10}$(body mass). Substitution rates were divided by 100 in the model. Maximum and minimum 95% CIs correspond to estimates made using 95% CI of molecular dating

Positions	Calibration sets	R^2	Mean Slope; intercept	Maximum 95% CI Slope; intercept	Minimum 95% CI Slope; intercept
3rd	2	0.46	−0.145; 0.459	−0.143; 0.559	−0.141; 0.367
3rd	4	0.60	−0.247; 0.813	−0.243; 0.905	−0.246; 0.730
All	2	0.35	−0.122; −0.185	−0.123; 0.076	−0.118; −0.274
All	4	0.51	−0.227; 0.177	−0.220; 0.266	−0.224; 0.089

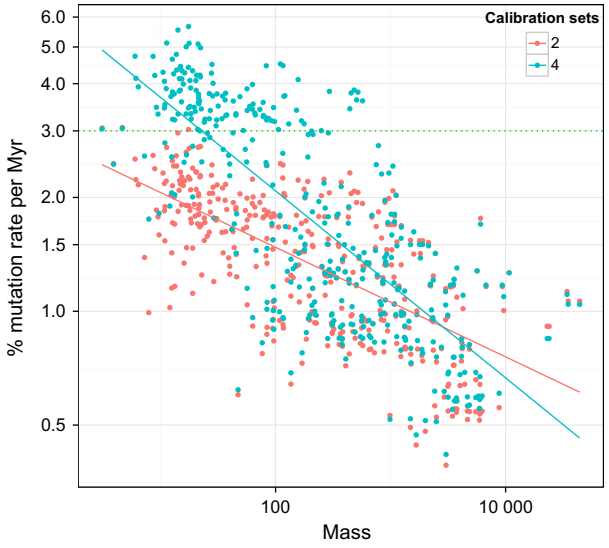

Fig. 1 Correlation between body mass and third codon position substitution rates. The dotted green line indicates an approximation of the rate corresponding to a 2% divergence per million years.

mass are presented in Table 3. These models allow us to predict a species' third codon mitochondrial substitution rate given its body mass using the following equation:

$$\text{Substitution rate} = \frac{10^{(\text{slope}\times\log_{10}(\text{Mass})+\text{intercept})}}{100}.$$

For example, using the parameters of analysis 2, a bird of 10 g (e.g. small passerines—some white eyes: Zosteropidae, sunbirds: Nectariniidae) is predicted to evolve at $(10^{(-0.145\times\log_{10}(10)+0.459)}/100)$ 0.0206 subst/site/Myr for third codon position. In contrast, birds of 1000 g such as the mallard (*Anas platyrhynchos*), the kelp gull (*Larus dominicanus*) or a medium-size raptors such as the crested serpent eagle (*Spilornis cheela*), for example, will evolve two times slower at 0.0106 subst/site/Myr for third codon position. These values convert to divergence rates of 4.2% and 2.1% per Myr, respectively. Analysis 4 gave linear models with steeper slopes than analysis 2, which creates a larger difference between the predicted substitution rates for any given pair of species. For example, in analysis 4, birds of 10 g and 1 kg are predicted to have substitution rates of 0.0368 and 0.0118 subst/site/Myr, respectively (7.4% and 2.4% divergence per Myr).

Finally, to take the uncertainty of molecular dating into account, we repeated the substitution rate estimation using calibration points taken from the minimum and the maximum 95% CIs of the estimated divergences dates. The maximum 95% CIs provide minimal divergence and, therefore, an estimated maximum for the substitution rate, whereas the minimum 95% CI dates provide a minimal substitution rate (Table 3).

Substitution rates differ among Protein-coding genes

For each of the protein-coding genes in our data set (except ND6, ND4L and ATP8), we estimated substitution rates from both third codon positions alone and all codon positions combined. The results from analyses 2 and 4 are qualitatively similar, so we only present the results from analysis 2 here. Using all codon positions, we detected significant variation in substitution rates among genes (linear model, gene effect: $P < 0.001$). COX1, COX2, COX3 and CYTB have a lower substitution rate than the ND genes and ATP6 (Fig. 2a, pairwise *t*-test). The fastest evolving gene (ND2, median rate = 0.0081) evolves, on average, 1.5 times faster than the slowest (COX2, median rate = 0.0055) (see Table S3, Supporting information for details).

Using third codon positions, we also detected significant variation in substitution rates among genes (linear model, gene effect: $P < 0.001$). As for all codon positions, COX proteins are generally slower than ND and ATP6 (Fig. 2b). The range of variation is lower, with the fastest gene (ND1, median rate = 0.0150) evolving 1.2 times faster than the slowest (COX3, median rate = 0.0121).

To take these variations into account, we computed the difference between the median rates of each gene individually with the full alignment (Table S4, Supporting information). These values could serve as correction factor to the mass-corrected substitutions when using reduced sets of genes.

Working examples

Circus harriers. We obtained the body mass of 14 of 16 species (*C. hudsonius* and *C. spilothorax* are missing) of harriers in the original data set. Body mass appears homogeneous in this clade (mean = 507 g, SD = 132 g) which is ideal to apply a single mass-corrected rate for the whole phylogeny. Moreover, the molecular divergence is moderate, with the maximal divergence between any two species at 14%. It is important to limit the divergence as third codon position can saturate rapidly due to their fast rate of evolution, leading to an inaccurate branch length estimates (Nguyen & Ho 2016). Using the parameters from Table 3, the mass-corrected substitution rates vary between 0.0116 (0.0097–0.0149) subst/sites/Myr for third codon position and 0.0140 (0.0116–0.0177) subst/sites/Myr for third codon position for the calibration sets 2 and 4, respectively. This rate leads to divergence dates that are approximately twice as old as the dates that would be obtained

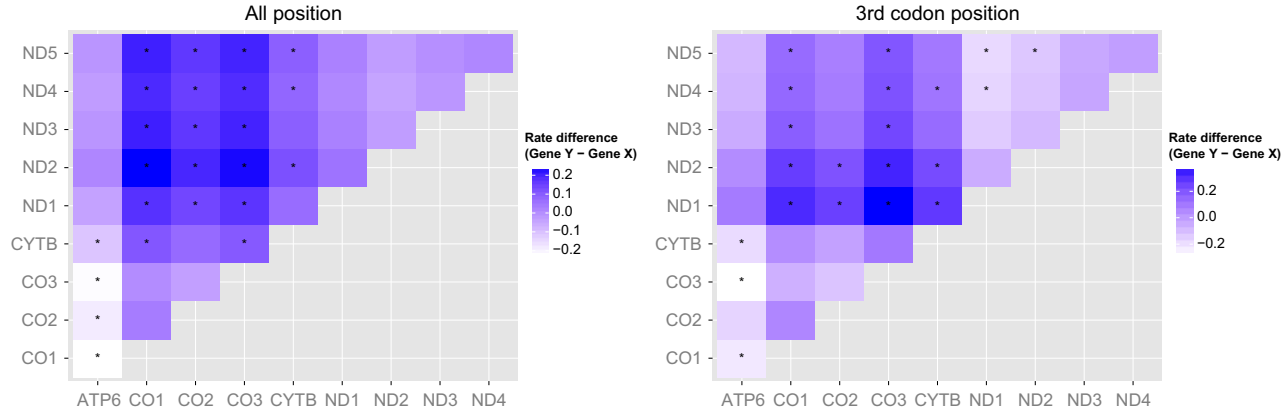

Fig. 2 Pairwise comparison of substitution rates between protein-coding genes. Colour indicates the direction and the intensity of the difference. A deep blue colour indicates that the gene on the *x*-axis evolves at a slower rate than the gene on the *y*-axis, whereas a white colour indicates the opposite. A star indicates when the difference is statistically significant (pairwise *t*-test with *P* value <0.01 after Bonferroni correction).

by assuming the widely used molecular clock rate of 2.1% divergence per Myr (Table 4). The first split within the genus (Node B) is estimated to have occurred at 10.3–15.8 Myr following by the diversification of 'steppe' harrier (nodes C, D and I; Oatley *et al.* 2015). Applying the gene-specific rate, the discrepancy would have been even greater because ND1 evolves 5–7.5% faster than the rate estimated with all the protein-coding genes (Table S3, Supporting information). Although much older, these dates are still largely in agreement with the appearance of open habitat and C4 grassland ecosystems during mid-Miocene (Edwards *et al.* 2010). Our estimates also support a recent origin of the Marsh harrier clades (Node E) of between 2.9 and 4.4 Myr.

Buff-throated Woodcreeper complex Xiphorhynchus. We obtained the body mass of six of seven species of *Xiphorhynchus* (*X. eytoni* is not available) in the original data set. The maximal molecular divergence between any two species is 12%. As for the harrier, the body mass appears very homogeneous in this clade (mean = 48.6 g, SD = 8.8 g). Using the parameters from Table 3, the mass-corrected substitution rates vary between 0.0163 (0.0135–0.0208) subst/sites/Myr for third codon position and 0.0249 (0.0207–0.0313) subst/sites/Myr for third codon position using calibration sets 2 and 4, respectively. The mass-corrected rate leads to divergence dates that are close to those obtained using the widely used divergence rate of 2.1% per Myr (Table 5) and, therefore, are largely congruent with the dates proposed in the original publication that include palaeontological and fossil calibrations as well as the molecular clock calibration (Rocha *et al.* 2015).

Table 4 Divergence times and confidence intervals according to body mass-corrected substitution rate (calibration sets 2 and 4) and to the 2.1% of divergence per Myr. The nodes are presented in fig. 2 of Oatley *et al.* (2015)

Node	2.1 % (±0.1%)	Calibration set 2	Calibration set 4
B	6.3 (6–6.6)	13.1 (10.3–15.8)	11 (8.7–13.2)
C	4.7 (4.5–4.9)	9.7 (7.6–11.6)	8.1 (6.4–9.7)
D	4.2 (4–4.4)	8.3 (6.5–10.1)	7 (5.5–8.4)
E	2 (1.9–2.1)	3.7 (2.9–4.4)	3.1 (2.4–3.7)
F	1.0 (0.9–1)	1.7 (1.3–2.0)	1.4 (1.1–1.7)
G	0.5 (0.5–0.6)	0.8 (0.6–0.9)	0.6 (0.5–0.8)
H	0.1 (0.1–0.1)	0.1 (0.1–0.2)	0.1 (0.1–0.1)
I	5.5 (5.2–5.7)	12 (9.4–14.5)	10.1 (7.9–12.1)
J	1.7 (1.7–1.8)	3.5 (2.7–4.2)	2.9 (2.3–3.5)
K	1.3 (1.2–1.4)	2.5 (1.9–3)	2.1 (1.6–2.5)
L	0.9 (0.9–1)	2.0 (1.5–2.4)	1.6 (1.3–2)

Discussion

In the present study, we propose a simple model to predict mitochondrial substitution rates from species' body mass. In line with several previous studies (Pereira & Baker 2006; Brown *et al.* 2008; Nabholz *et al.* 2009; Eo & DeWoody 2010; Lanfear *et al.* 2010; Pacheco

Table 5 Divergence times and confidence intervals according to body mass-corrected substitution rate (calibration sets 2 and 4) and to the 2.1% of divergence per Myr. The nodes are presented in fig. 3 of Rocha *et al.* (2015)

Node	2.1% (±0.1%)	Calibration set 2	Calibration set 4
I	3.9 (3.8–4.1)	6.0 (4.7–7.3)	3.9 (3.1–4.7)
II	3.4 (3.2–3.6)	5.4 (4.2–6.5)	3.5 (2.8–4.2)
III	2.2 (2.1–2.3)	3.1 (2.5–3.8)	2.1 (1.7–2.5)
IV	1.3 (1.2–1.3)	2.1 (1.7–2.6)	1.4 (1.1–1.7)
V	0.4 (0.4–0.5)	0.6 (0.5–0.7)	0.4 (0.3–0.5)

et al. 2011), we detected extensive and statistically significant variation in substitution rates among bird species. Using body mass alone, we were able to predict up to 60% of the variation in observed substitution rates, suggesting that using body mass-corrected molecular rates is superior to a strict molecular clock approach.

The extensive substitution rate variation we describe is smaller than the one reported by Nabholz *et al.* (2009). Nabholz *et al.* (2009) reported a median of 0.018 subst/sites/Myr with a variation from 0.003 and 0.09 subst/sites/Myr. This discrepancy could simply be explained by the fact that Nabholz *et al.* (2009) used only CYTB for molecular dating and substitution rate estimation in contrast to all the H-strand encoded protein-coding genes, therefore leading to higher sampling variance in the substitution process in the earlier study.

Our estimates of mitochondrial substitution rates are often lower than the commonly used divergence rate of 2% per million years, although they are largely concordant with the estimates of Pereira & Baker (2006) (range from 0.0009 to 0.012 subst/sites/Myr) and Pacheco *et al.* (2011) (average rate per genes range from 0.0027 to 0.0068 subst/sites/Myr). It was only in the analysis constraining the divergence between the Oscines and Suboscines to be younger than 34 Myr (analysis 4) that a substantial number of species (mostly passerines) have a divergence rates close to or above 2% per million years. The discrepancy between the analyses reflects the current uncertainty surrounding fossils calibrations used to estimate the timescale of avian diversification (Mayr 2013; Cracraft *et al.* 2015; Mitchell *et al.* 2015). For example, analyses with calibration sets 1, 2 and 3 provide an age for the Oscines/Suboscines divergence that is 30–35 Myr years older than the fossil record. This discrepancy may seem surprising because no stem Passeriformes are known from the Paleocene, let alone the derived Oscines and Suboscines representatives (Mayr 2009). However, the fossil record of passerines could be biased towards missing the earliest fossils, because most known deposits exist in the Northern Hemisphere, whereas both crown and stem Passeriformes likely originated in the Southern Hemisphere (Boles 1997; Ericson *et al.* 2002). Our analyses 1, 2, and 3 suggest that the diversification of Hawaiian Honeycreepers pre-dates the oldest Hawaiian island (Kauai–Niihau). Thus, our analyses support either that the diversification started before the emergence of the oldest island or that at least two independent colonization events have occurred. Both scenarios are possible as older islands existed before Kauai–Niihau (Price & Clague 2002) and many examples of old taxa on young islands are known (Heads 2011), although the latter could also result from the extinction of the mainland sister taxa.

Our analyses show that the correlations between body mass and substitution rates are stronger when substitution rates are estimated exclusively from third codon positions. This could be because third codon positions are less affected by natural selection than first and second codon positions. Selective constraint acting on mitochondrial genes is known to be associated with speed of movement (Shen *et al.* 2009) and island/mainland status (Johnson & Seger 2001; Woolfit & Bromham 2005), a variable related to the effective population size. Positive selection has also been detected in vertebrate mitochondrial evolution (Grossman *et al.* 2004; Castoe *et al.* 2008, 2009) although not, to date, in birds. Positive selection could episodically inflate the substitution rate. Regardless of the reason for the difference in the strength of association between body mass and substitution rate estimates, we suggest using molecular rates estimated from third codon positions when using body mass-corrected molecular rates, as it is these rates which can be most accurately predicted from body mass data. Our analyses reveal significant variation in substitution rates among mitochondrial protein-coding genes. Using substitution rates estimated from all codon positions, we show that NADH-dehydrogenase (ND, proteins of the complex I) genes evolved faster than cytochrome oxidase (COX, proteins of the complex IV) and CYTB genes. These results are in line with those of Eo & DeWoody (2010), Smith & Klicka (2010), Pacheco *et al.* (2011), Lerner *et al.* (2011) and Nguyen & Ho (2016). Eo & DeWoody (2010) and Pacheco *et al.* (2011) report a variation among genes that is higher than in our analysis (e.g. ND2 being 2.2 times faster than COX1 in Pacheco *et al.* 2011). Using data sets composed of passerines, Nguyen & Ho (2016) also detected fast evolution for ND genes; however, CYTB was reported as clearly the slowest genes which is not the case in our analysis. The observed variation might be a consequence of the variation in evolutionary constraint among genes, as the ND genes are known to be less constrained than the COX genes (Mishmar *et al.* 2003; Nabholz *et al.* 2013). Interestingly, we also detected extensive variation of third codon position substitution rates among protein-coding genes. The variation among genes could be explained in two ways: (i) a difference in mutation rate among genes and (ii) selection acting on synonymous sites. Neither GC content nor the positions of the protein in the genome (that is linked to the time spend single stranded during, Reyes *et al.* 1998) explain the observed difference in substitution rate among genes. Selection on synonymous sites is a possibility, for example, through a selection on codon usage driven by the large variation in expression level among protein-coding genes (Nabholz *et al.* 2013). Additionally, indirect evidence of selection on synonymous sites is also provided by mutations linked to human disease. Among the 271

point mutations located within the protein-coding genes that are known to cause diseases in humans, nine are synonymous mutations (Lott *et al.* 2013).

Finally, we reanalysed two data sets to illustrate the principle of our method. These analyses show that in some cases, particularly with nonpasserine birds, the assumption of the widely used divergence rate of 2% per million years can give very different answers from using the body mass-corrected molecular rates we derive here. We emphasis three additional points as a guideline to users of our corrected molecular rates. First, the species analysed should have a limited molecular divergence. An arbitrary threshold could be a pairwise molecular divergence below 1.0 subst/site for the third codon position, which corresponds to a divergence of 0.3–0.4 subst/site (i.e. 30–40% divergence) for all codon position. When divergence is higher, we recommend splitting the data set into smaller clades and analysing each clade independently. Second, when few loci are available, overparametrization of the model of molecular evolution could be an issue. Particularly, we noted that the kappa parameter in our empirical analyses increased to unrealistic values (>100) in some small data sets, leading to unrealistically inflated branch length estimates. We therefore recommend fixing this parameter to a reasonable value a priori—the one estimated using all codon positions—when only a few loci are available for analysis. Third, the within-clade body mass should be rather homogeneous among the species of a clade (this is likely when analysing clades of limited molecular divergence). This will help to ensure that applying a single correction factor the molecular branch lengths is warranted. If body mass varies widely within a clade, the substitution rate is unlikely to be accurately approximated using a single molecular clock estimated from the average body mass of that clade. In this case, we also recommend splitting the data set into monophyletic clades of species with relatively homogeneous body mass, and analysing each clade independently.

Acknowledgements

We thank Loïs Rancilhac and Florent Sylvestre for their help during preliminary analysis. We also thank the four anonymous reviewers for their comments and corrections. This work was supported by Agence Nationale de la Recherche grants ANR-14-CE02-0002-01 'BirdIslandGenomic' to B. N. This is ISEM publication number ISEM 2016-147.

References

Avise JC, Walker DE (1998) Pleistocene phylogeographic effects on avian populations and the speciation process. *Proceedings of the Royal Society of London B: Biological Sciences*, **265**, 457–463.

Benton MJ, Donoghue PCJ, Asher RJ (2009) Calibrating and constraining molecular clocks. *The timetree of life*, 35–86.

Boles WE (1997) Fossil songbirds (Passeriformes) from the early Eocene of Australia. *Emu*, **97**, 43–50.

Bromham L (2009) Why do species vary in their rate of molecular evolution? *Biology Letters*, **5**, 401–404.

Bromham L, Rambaut A, Harvey PH (1996) Determinants of rate variation in mammalian DNA sequence evolution. *Journal of Molecular Evolution*, **43**, 610–621.

Brown WM, George M, Wilson AC (1979) Rapid evolution of animal mitochondrial DNA. *Proceedings of the National Academy of Sciences*, **76**, 1967–1971.

Brown WM, Prager EM, Wang A, Wilson AC (1982) Mitochondrial DNA sequences of primates: tempo and mode of evolution. *Journal of Molecular Evolution*, **18**, 225–239.

Brown JW, Rest JS, García-Moreno J, Sorenson MD, Mindell DP (2008) Strong mitochondrial DNA support for a Cretaceous origin of modern avian lineages. *BMC Biology*, **6**, 6.

Campbell KE, Marcus L (1992) The relationships of hindlimb bone dimensions to body weight in birds. In: *Papers in Avian Paleontology Honoring Pierce Brodkorb. Science Series 36*. (ed. Campbell KE Jr.), pp. 395–412. Natural History Museum of Los Angeles County, Los Angeles.

Castoe TA, Jiang ZJ, Gu W, Wang ZO, Pollock DD (2008) Adaptive evolution and functional redesign of core metabolic proteins in snakes. *PLoS One*, **3**, e2201.

Castoe TA, de Koning APJ, Kim H-M *et al.* (2009) Evidence for an ancient adaptive episode of convergent molecular evolution. *Proceedings of the National Academy of Sciences, USA*, **106**, 8986–8991.

Cracraft J, Houde P, Ho SYW *et al.* (2015) Response to Comment on "Whole-genome analyses resolve early branches in the tree of life of modern birds". *Science*, **349**, 1460.

Dunning JBJ (2007) *CRC Handbook of Avian Body Masses*, 2nd edn. CRC Press, Boca Raton, Florida.

Edgar RC (2004) MUSCLE: a multiple sequence alignment method with reduced time and space complexity. *BMC Bioinformatics*, **5**, 113.

Edwards EJ, Osborne CP, Strömberg CAE, Smith SA, Consortium CG (2010) The origins of C4 grasslands: integrating evolutionary and ecosystem science. *Science*, **328**, 587–591.

Eo SH, DeWoody JA (2010) Evolutionary rates of mitochondrial genomes correspond to diversification rates and to contemporary species richness in birds and reptiles. *Proceedings of the Royal Society of London B: Biological Sciences*, **277**, 3587–3592.

Ericson PG, Christidis L, Cooper A *et al.* (2002) A Gondwanan origin of passerine birds supported by DNA sequences of the endemic New Zealand wrens. *Proceedings of the Royal Society of London B: Biological Sciences*, **269**, 235–241.

Felsenstein J (1974) The evolutionary advantage of recombination. *Genetics*, **78**, 737–756.

Field DJ, Lynner C, Brown C, Darroch SA (2013) Skeletal correlates for body mass estimation in modern and fossil flying birds. *PLoS One*, **8**, e82000.

Fleischer RC, McIntosh CE, Tarr CL (1998) Evolution on a volcanic conveyor belt: using phylogeographic reconstructions and K-Ar-based ages of the Hawaiian Islands to estimate molecular evolutionary rates. *Molecular Ecology*, **7**, 533–545.

García-Moreno J (2004) Is there a universal mtDNA clock for birds? *Journal of Avian Biology*, **35**, 465–468.

Garland JT, Ives AR, Travis EJ, Pagel AEM (2000) Using the past to predict the present: confidence intervals for regression equations in phylogenetic comparative methods. *The American Naturalist*, **155**, 346–364.

Gibb GC, England R, Hartig G *et al.* (2015) New Zealand passerines help clarify the diversification of major songbird lineages during the oligocene. *Genome Biology and Evolution*, **11**, 2983–2995.

Grafen A (1989) The phylogenetic regression. *Philosophical Transactions of the Royal Society of London. Series B, Biological Sciences*, **326**, 119–157.

Grossman LI, Wildman DE, Schmidt TR, Goodman M (2004) Accelerated evolution of the electron transport chain in anthropoid primates. *Trends in Genetics*, **20**, 578–585.

Hall TA (1999) BioEdit: a user-friendly biological sequence alignment editor and analysis program for Windows 95/98/NT. *Nucleic Acids Symposium Series*, **41**, 95–98.

Heads M (2005) Dating nodes on molecular phylogenies: a critique of molecular biogeography. *Cladistics*, **21**, 62–78.

Heads M (2011) Old taxa on young islands: a critique of the use of island age to date island-endemic clades and calibrate phylogenies. *Systematic Biology*, **60**, 204–218.

Ho SYM (2007) Calibrating molecular estimates of substitution rates and divergence times in birds. *Journal of Avian Biology*, **38**, 409–414.

Jarvis ED, Mirarab S, Aberer AJ *et al.* (2014) Whole-genome analyses resolve early branches in the tree of life of modern birds. *Science*, **346**, 1320–1331.

Jetz W, Thomas GH, Joy JB, Hartmann K, Mooers AO (2012) The global diversity of birds in space and time. *Nature*, **491**, 444–448.

Johnson KP, Seger J (2001) Elevated rates of nonsynonymous substitution in island birds. *Molecular Biology and Evolution*, **18**, 874–881.

Ksepka D, Clarke JA (2015) Phylogenetically vetted and stratigraphically constrained fossil calibrations within Aves. *Palaeontologia Electronica*, **18**, 1–25.

Lanfear R, Ho SYW, Love D, Bromham L (2010) Mutation rate is linked to diversification in birds. *Proceedings of the National Academy of Sciences*, **107**, 20423–20428.

Lartillot N, Lepage T, Blanquart S (2009) PhyloBayes 3: a Bayesian software package for phylogenetic reconstruction and molecular dating. *Bioinformatics*, **25**, 2286–2288.

Lehtonen J, Lanfear R (2014) Generation time, life history and the substitution rate of neutral mutations. *Biology Letters*, **10**, 20140801.

Lepage T, Bryant D, Philippe H, Lartillot N (2007) A general comparison of relaxed molecular clock models. *Molecular Biology and Evolution*, **24**, 2669–2680.

Lerner HRL, Meyer M, James HF, Hofreiter M, Fleischer RC (2011) Multilocus resolution of phylogeny and timescale in the extant adaptive radiation of Hawaiian honeycreepers. *Current Biology*, **21**, 1838–1844.

Longrich NR, Tokaryk T, Field DJ (2011) Mass extinction of birds at the Cretaceous-Paleogene (K-Pg) boundary. *Proceedings of the National Academy of Sciences*, **108**, 15253–15257.

Lott MT, Leipzig JN, Derbeneva O *et al.* (2013) mtDNA variation and analysis using MITOMAP and MITOMASTER. *Current Protocols in Bioinformatics*, **44**, 1–23.

Lourenço JM, Glémin S, Chiari Y, Galtier N (2013) The determinants of the molecular substitution process in turtles. *Journal of Evolutionary Biology*, **26**, 38–50.

Lovette IJ (2004) Mitochondrial dating and mixed support for the "2% rule" in birds. *The Auk*, **121**, 1–6.

Manegold A (2007) Earliest fossil record of the Certhioidea (treecreepers and allies) from the early Miocene of Germany. *Journal of Ornithology*, **149**, 223–228.

Mayr G (2009) *Paleogene Fossil Birds*. Springer, Heidelberg.

Mayr G (2013) The age of the crown group of passerine birds and its evolutionary significance–molecular calibrations versus the fossil record. *Systematics and Biodiversity*, **11**, 7–13.

Mayr G, Manegold A (2004) The oldest European fossil songbird from the early oligocene of Germany. *Naturwissenschaften*, **91**, 173–177.

Mayr G, Manegold A (2006) A small suboscine-like passeriform bird from the early oligocene of France. *The Condor*, **108**, 717.

Mishmar D, Ruiz-Pesini E, Golik P *et al.* (2003) Natural selection shaped regional mtDNA variation in humans. *Proceedings of the National Academy of Sciences, USA*, **100**, 171–176.

Mitchell KJ, Cooper A, Phillips MJ (2015) Comment on "Whole-genome analyses resolve early branches in the tree of life of modern birds". *Science*, **349**, 1460.

Nabholz B, Glémin S, Galtier N (2008) Strong variations of mitochondrial mutation rate across mammals–the longevity hypothesis. *Molecular Biology and Evolution*, **25**, 120–130.

Nabholz B, Glémin S, Galtier N (2009) The erratic mitochondrial clock: variations of mutation rate, not population size, affect mtDNA diversity across birds and mammals. *BMC Evolutionary Biology*, **9**, 54.

Nabholz B, Ellegren H, Wolf JBW (2013) High levels of gene expression explain the strong evolutionary constraint of mitochondrial protein-coding genes. *Molecular Biology and Evolution*, **30**, 272–284.

Nguyen JMT, Ho SYW (2016) Mitochondrial rate variation among lineages of passerine birds. *Journal of Avian Biology*, **22**, 1561–1568.

Oatley G, Simmons RE, Fuchs J (2015) A molecular phylogeny of the harriers (Circus, Accipitridae) indicate the role of long distance dispersal and migration in diversification. *Molecular Phylogenetics and Evolution*, **85**, 150–160.

Pacheco MA, Battistuzzi FU, Lentino M *et al.* (2011) Evolution of modern birds revealed by mitogenomics: timing the radiation and origin of major orders. *Molecular Biology and Evolution*, **28**, 1927–1942.

Paradis E (2011) *Analysis of Phylogenetics and Evolution with R*. Springer, New York.

Pereira SL, Baker AJ (2006) A mitogenomic timescale for birds detects variable phylogenetic rates of molecular evolution and refutes the standard molecular clock. *Molecular Biology and Evolution*, **23**, 1731–1740.

Popescu A-A, Huber KT, Paradis E (2012) APE 3.0: new tools for distance-based phylogenetics and evolutionary analysis in R. *Bioinformatics*, **28**, 1536–1537.

Price JP, Clague DA (2002) How old is the Hawaiian biota? Geology and phylogeny suggest recent divergence. *Proceedings of the Royal Society of London B: Biological Sciences*, **269**, 2429–2435.

Prum RO, Berv JS, Dornburg A *et al.* (2015) A comprehensive phylogeny of birds (Aves) using targeted next-generation DNA sequencing. *Nature*, **526**, 569–573.

Qiu F, Kitchen A, Burleigh JG, Miyamoto MM (2014) Scombroid fishes provide novel insights into the trait/rate associations of molecular evolution. *Journal of Molecular Evolution*, **78**, 338–348.

R Core Team (2013) *R: A Language and Environment for Statistical Computing*. R Development Core Team, Vienna, Austria.

Rannala B, Yang Z (2007) Inferring speciation times under an episodic molecular clock. *Systematic Biology*, **56**, 453–466.

Reyes A, Gissi C, Pesole G, Saccone C (1998) Asymmetrical directional mutation pressure in the mitochondrial genome of mammals. *Molecular Biology and Evolution*, **15**, 957–966.

Rocha TC, Sequeira F, Aleixo A *et al.* (2015) Molecular phylogeny and diversification of a widespread Neotropical rainforest bird group: the Buff-throated Woodcreeper complex, *Xiphorhynchus guttatus*/susurrans (Aves: Dendrocolaptidae). *Molecular Phylogenetics and Evolution*, **85**, 131–140.

Shen Y-Y, Shi P, Sun Y-B, Zhang Y-P (2009) Relaxation of selective constraints on avian mitochondrial DNA following the degeneration of flight ability. *Genome Research*, **19**, 1760–1765.

Shields GF, Wilson AC (1987) Calibration of mitochondrial DNA evolution in geese. *Journal of Molecular Evolution*, **24**, 212–217.

Smith A (2015) Fifteen vetted fossil calibrations for divergence dating of Charadriiformes (Aves, Neognathae). *Palaeontologia Electronica*, **18**, 1–18.

Smith BT, Klicka J (2010) The profound influence of the Late Pliocene Panamanian uplift on the exchange, diversification, and distribution of New World birds. *Ecography*, **33**, 333–342.

Stamatakis A (2014) RAxML version 8: a tool for phylogenetic analysis and post-analysis of large phylogenies. *Bioinformatics*, **30**, 1312–1313.

Thomas JA, Welch JJ, Lanfear R, Bromham L (2010) A generation time effect on the rate of molecular evolution in invertebrates. *Molecular Biology and Evolution*, **27**, 1173–1180.

Thorne JL, Kishino H, Painter IS (1998) Estimating the rate of evolution of the rate of molecular evolution. *Molecular Biology and Evolution*, **15**, 1647–1657.

Trewick SA, Gibb GC (2010) Vicars, tramps and assembly of the New Zealand avifauna: a review of molecular phylogenetic evidence. *Ibis*, **152**, 226–253.

Weir JT, Schluter D (2008) Calibrating the avian molecular clock. *Molecular Ecology*, **17**, 2321–2328.

Weir JT, Bermingham E, Schluter D (2009) The Great American Biotic Interchange in birds. *Proceedings of the National Academy of Sciences, USA*, **106**, 21737–21742.

Welch J, Bininda-Emonds O, Bromham L (2008) Correlates of substitution rate variation in mammalian protein-coding sequences. *BMC Evolutionary Biology*, **8**, 53.

Woolfit M, Bromham L (2005) Population size and molecular evolution on islands. *Proceedings Biological Sciences/The Royal Society*, **272**, 2277–2282.

Yang Z (2007) PAML 4: phylogenetic analysis by maximum likelihood. *Molecular Biology and Evolution*, **24**, 1586–1591.

Yang Z, Rannala B (2006) Bayesian estimation of species divergence times under a molecular clock using multiple fossil calibrations with soft bounds. *Molecular Biology and Evolution*, **23**, 212–226.

B.N. initiated the study. All authors designed the study. J.F. created the dataset. B.N. and R.L. analysed the data. B.N. wrote the initial manuscript. All authors contributed to writing the manuscript and approved the final version.

Data accessibility

Alignments, phylogeny and body mass data for the main data set, the two working examples and R script to compute the molecular date using species body mass: Dryad doi: 10.5061/dryad.1040d.

Supporting information

Additional supporting information may be found in the online version of this article.

Fig. S1 Schematic descriptions of two-steps method.

Table S1 Taxa, body mass, sequences GenBank accession number and their references.

Table S2 Substitution rates for the third-codon (3rd) position and the full sequence (All) estimated using calibration sets 2 and 4.

Table S3 Correlation between third-codon position substitution rates and body-mass assessed by phylogenetic generalized least squares (PGLS) and phylogenetic independent contrast (PIC). Both variables are $\log_{10}$ transformed.

Table S4 Gene-specific substitution rates.